ACTION RECOGNITION USING VISUAL ATTENTION

Shikhar Sharma, Ryan Kiros & Ruslan Salakhutdinov
Department of Computer Science
University of Toronto
Toronto, ON M5S 3G4, Canada
{shikhar,rkiros,rsalakhu}@cs.toronto.edu

ABSTRACT

We propose a soft attention based model for the task of action recognition in videos. We use multi-layered Recurrent Neural Networks (RNNs) with Long Short-Term Memory (LSTM) units which are deep both spatially and temporally. Our model learns to focus selectively on parts of the video frames and classifies videos after taking a few glimpses. The model essentially learns which parts in the frames are relevant for the task at hand and attaches higher importance to them. We evaluate the model on UCF-11 (YouTube Action), HMDB-51 and Hollywood2 datasets and analyze how the model focuses its attention depending on the scene and the action being performed.

1 INTRODUCTION

It has been noted in visual cognition literature that humans do not focus their attention on an entire scene at once (Rensink, 2000). Instead, they focus sequentially on different parts of the scene to extract relevant information. Most traditional computer vision algorithms do not employ attention mechanisms and are indifferent to various parts of the image/video. With the recent surge of interest in deep neural networks, attention based models have been shown to achieve promising results on several challenging tasks, including caption generation (Xu et al., 2015), machine translation (Bahdanau et al., 2015), game-playing and tracking (Mnih et al., 2014), as well as image recognition (e.g. Street View House Numbers dataset (Ba et al., 2015b)). Many of these models have employed LSTM (Hochreiter & Schmidhuber, 1997) based RNNs and have shown good results in learning sequences.

Attention models can be classified into soft attention and hard attention models. Soft attention models are deterministic and can be trained using backpropagation, whereas hard attention models are stochastic and can be trained by the REINFORCE algorithm (Williams, 1992; Mnih et al., 2014), or by maximizing a variational lower bound or using importance sampling (Ba et al., 2015b;a). Learning hard attention models can become computationally expensive as it requires sampling. In soft attention approaches, on the other hand, a differentiable mapping can be used from all the locations output to the next input. Attention based models can also potentially infer the action happening in videos by focusing only on the relevant places in each frame. For example, Fig. 1a shows four frames from the UCF-11 video sequence belonging to the "golf swinging" category. The model tends to focus on the ball, the club, and the human, which allows the model to correctly recognize the activity as "golf swinging". In Fig. 1b, our model attends to the trampoline, while correctly identifying the activity as "trampoline jumping".

In this paper we propose a soft attention based recurrent model for action recognition. We describe how our model dynamically pools convolutional features and show that using these features for action recognition gives better results compared to average or max pooling which is used by many of the existing models (Zha et al., 2015). We further demonstrate that our model tends to recognize important elements in video frames based on the activities it detects.

2 RELATED WORK

Convolutional Neural Networks (CNNs) have been highly successful in image classification and object recognition tasks (Ren et al., 2015; Wu et al., 2015). Classifying videos instead of images

(a) Correctly classified as "golf swinging"   (b) Correctly classified as "trampoline jumping"
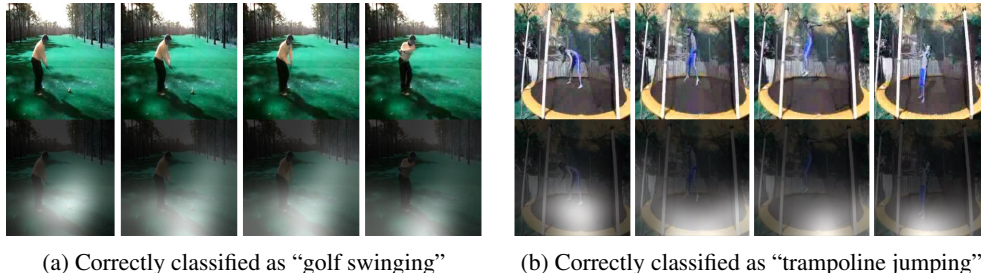
Figure 1: Attention over time: The white regions show what the model is attending to and the brightness indicates the strength of focus. Best viewed in color.

adds a temporal dimension to the problem of image classification. Learning temporal dynamics is a difficult problem and earlier approaches have used optical flow, HOG and hand-crafted features to generate descriptors with both appearance and dynamics information encoded. LSTMs have been recently shown to perform well in the domain of speech recognition (Graves et al., 2013), machine translation (Sutskever et al., 2014), image description (Xu et al., 2015; Vinyals et al., 2015) and video description (Yao et al., 2015; Venugopalan et al., 2014). They have also started picking up momentum in action recognition (Srivastava et al., 2015; Ng et al., 2015).

Most of the existing approaches also tend to have CNNs underlying the LSTMs and classify sequences directly or do temporal pooling of features prior to classification (Donahue et al., 2015; Ng et al., 2015). LSTMs have also been used to learn an effective representation of videos in unsupervised settings (Srivastava et al., 2015) by using them in an encoder-decoder framework. More recently, Yao et al. (2015) have proposed to use 3-D CNN features and an LSTM decoder in an encoder-decoder framework to generate video descriptions. Their model incorporates attention on a video level by defining a probability distribution over frames used to generate individual words. They, however, do not employ an attention mechanism on a frame level (i.e. within a single frame).

In general, it is rather difficult to interpret internal representations learned by deep neural networks. Attention models add a dimension of interpretability by capturing where the model is focusing its attention when performing a particular task. Karpathy et al. (2014) used a multi-resolution CNN architecture to perform action recognition in videos. They mention the concept of fovea but they fix attention to the center of the frame. A recent work of Xu et al. (2015) used both soft attention and hard attention mechanisms to generate image descriptions. Their model actually looks at the respective objects when generating their description. Our work directly builds upon this work. However, while Xu et al. (2015) primarily worked on caption generation in static images, in this paper, we focus on using a soft attention mechanism for activity recognition in videos. More recently, Jaderberg et al. (2015) have proposed a soft-attention mechanism called the *Spatial Transformer* module which they add between the layers of CNNs. Instead of weighting locations using a softmax layer which we do, they apply affine transformations to multiple layers of their CNN to attend to the relevant part and get state-of-the-art results on the Street View House Numbers dataset (Netzer et al., 2011). Yeung et al. (2015) do dense action labelling using a temporal attention based model on the input-output context and report higher accuracy and better understanding of temporal relationships in action videos.

3 THE MODEL AND THE ATTENTION MECHANISM

3.1 CONVOLUTIONAL FEATURES

We extract the last convolutional layer obtained by pushing the video frames through GoogLeNet model (Szegedy et al., 2015) trained on the ImageNet dataset (Deng et al., 2009). This last convolutional layer has D convolutional maps and is a feature cube of shape $K \times K \times D$ ($7 \times 7 \times 1024$ in our experiments). Thus, at each time-step t, we extract K^2 D-dimensional vectors. We refer to these vectors as feature slices in a feature cube:

$$\mathbf{X}_t = [\mathbf{X}_{t,1}, \dots, \mathbf{X}_{t,K^2}], \qquad\qquad \mathbf{X}_{t,i} \in \mathbb{R}^D.$$

Each of these K^2 vertical feature slices maps to different overlapping regions in the input space and our model chooses to focus its attention on these K^2 regions.

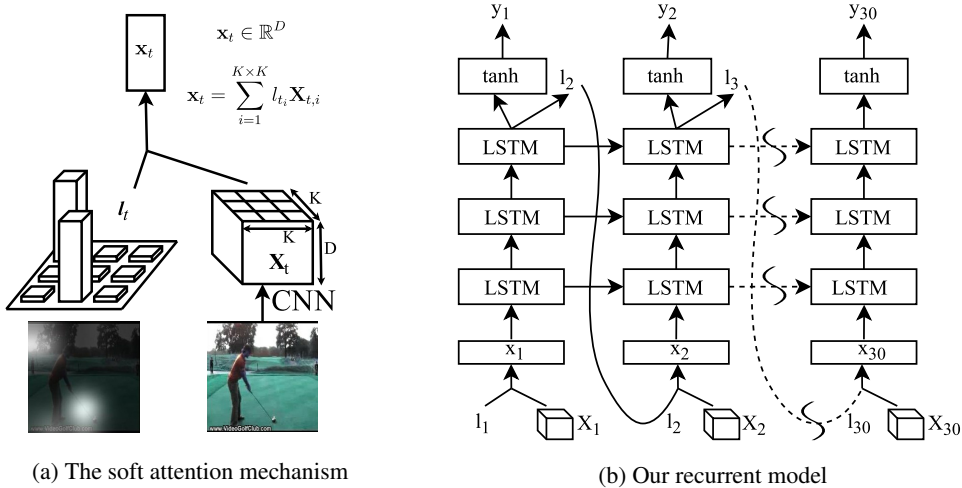(a) The soft attention mechanism

(b) Our recurrent model

Figure 2: (2a) The CNN takes the video frame as its input and produces a feature cube. The model computes the current input $\mathbf{x}_t$ as an average of the feature slices weighted according to the location softmax $\mathbf{l}_t$ (2b) At each time-step t, our recurrent network takes a feature slice $\mathbf{x}_t$, generated as in (2a), as the input. It then propagates $\mathbf{x}_t$ through three layers of LSTMs and predicts the next location probabilities $\mathbf{l}_{t+1}$ and the class label $\mathbf{y}_t$.

3.2 THE LSTM AND THE ATTENTION MECHANISM

We use the LSTM implementation discussed in Zaremba et al. (2014) and Xu et al. (2015):

$$\begin{pmatrix} \mathbf{i}_t \\ \mathbf{f}_t \\ \mathbf{o}_t \\ \mathbf{g}_t \end{pmatrix} = \begin{pmatrix} \sigma \\ \sigma \\ \sigma \\ \tanh \end{pmatrix} M \begin{pmatrix} \mathbf{h}_{t-1}, \\ \mathbf{x}_t \end{pmatrix}, \tag{1}$$

$$\mathbf{c}_t = \mathbf{f}_t \odot \mathbf{c}_{t-1} + \mathbf{i}_t \odot \mathbf{g}_t, \tag{2}$$

$$\mathbf{h}_t = \mathbf{o}_t \odot \tanh(\mathbf{c}_t), \tag{3}$$

where $\mathbf{i}_t$ is the input gate, $\mathbf{f}_t$ is the forget gate, $\mathbf{o}_t$ is the output gate, and $\mathbf{g}_t$ is calculated as shown in Eq. 1. $\mathbf{c}_t$ is the cell state, $\mathbf{h}_t$ is the hidden state, and $\mathbf{x}_t$ (see Eqs. 4, 5) represents the input to the LSTM at time-step t. $M : \mathbb{R}^a \to \mathbb{R}^b$ is an affine transformation consisting of trainable parameters with $a = d + D$ and $b = 4d$, where d is the dimensionality of all of $\mathbf{i}_t, \mathbf{f}_t, \mathbf{o}_t, \mathbf{g}_t, \mathbf{c}_t$, and $\mathbf{h}_t$.

At each time-step t, our model predicts $\mathbf{l}_{t+1}$, a softmax over $K \times K$ locations, and $\mathbf{y}_t$, a softmax over the label classes with an additional hidden layer with $tanh$ activations (see Fig. 2b). The location softmax is defined as follows:

$$l_{t,i} = p(\mathbf{L}_t = i | \mathbf{h}_{t-1}) = \frac{\exp(W_i^\top \mathbf{h}_{t-1})}{\sum_{j=1}^{K \times K} \exp(W_j^\top \mathbf{h}_{t-1})} \qquad i \in 1 \ldots K^2, \tag{4}$$

where W_i are the weights mapping to the ith element of the location softmax and $\mathbf{L}_t$ is a random variable which can take 1-of-K^2 values. This softmax can be thought of as the probability with which our model believes the corresponding region in the input frame is important. After calculating these probabilities, the soft attention mechanism (Bahdanau et al., 2015) computes the expected value of the input at the next time-step $\mathbf{x}_t$ by taking expectation over the feature slices at different regions (see Fig. 2a):

$$\mathbf{x}_t = \mathbb{E}_{p(\mathbf{L}_t|\mathbf{h}_{t-1})}[\mathbf{X}_t] = \sum_{i=1}^{K^2} l_{t,i} \mathbf{X}_{t,i}, \tag{5}$$

where $\mathbf{X}_t$ is the feature cube and $\mathbf{X}_{t,i}$ is the ith slice of the feature cube at time-step t. Note that in the hard attention based models, we would sample $\mathbf{L}_t$ from a softmax distribution of Eq. 4. The input $\mathbf{x}_t$ would then be the feature slice at the sampled location instead of taking expectation over all the slices. Thus, hard attention based models are not differentiable and have to resort to some form of sampling.

We use the following initialization strategy (see Xu et al. (2015)) for the cell state and the hidden state of the LSTM for faster convergence:

$$\mathbf{c}_0 = f_{\text{init,c}} \left(\frac{1}{T} \sum_{t=1}^{T} \left(\frac{1}{K^2} \sum_{i=1}^{K^2} \mathbf{X}_{t,i} \right) \right) \quad \text{and} \quad \mathbf{h}_0 = f_{\text{init,h}} \left(\frac{1}{T} \sum_{t=1}^{T} \left(\frac{1}{K^2} \sum_{i=1}^{K^2} \mathbf{X}_{t,i} \right) \right), \quad (6)$$

where $f_{\text{init,c}}$ and $f_{\text{init,h}}$ are two multilayer perceptrons and T is the number of time-steps in the model. These values are used to calculate the first location softmax $\mathbf{l}_1$ which determines the initial input $\mathbf{x}_1$. In our experiments, we use multi-layered deep LSTMs, as shown in Fig. 2b.

3.3 LOSS FUNCTION AND THE ATTENTION PENALTY

We use cross-entropy loss coupled with the doubly stochastic penalty introduced in Xu et al. (2015). We impose an additional constraint over the location softmax, so that $\sum_{t=1}^{T} l_{t,i} \approx 1$. This is the attention regularization which forces the model to look at each region of the frame at some point in time. The loss function is defined as follows:

$$L = -\sum_{t=1}^{T} \sum_{i=1}^{C} y_{t,i} \log \hat{y}_{t,i} + \lambda \sum_{i=1}^{K^2} (1 - \sum_{t=1}^{T} l_{t,i})^2 + \gamma \sum_i \sum_j \theta_{i,j}^2, \quad (7)$$

where y_t is the one hot label vector, $\hat{y}_t$ is the vector of class probabilities at time-step t, T is the total number of time-steps, C is the number of output classes, λ is the attention penalty coefficient, γ is the weight decay coefficient, and θ represents all the model parameters. Details about the architecture and hyper-parameters are given in Section 4.2.

4 EXPERIMENTS

4.1 DATASETS

We have used UCF-11, HMDB-51 and Hollywood2 datasets in our experiments. UCF-11 is the YouTube Action dataset consisting of 1600 videos and 11 actions - basketball shooting, biking/cycling, diving, golf swinging, horse back riding, soccer juggling, swinging, tennis swinging, trampoline jumping, volleyball spiking, and walking with a dog. The clips have a frame rate of 29.97 fps and each video has only one action associated with it. We use 975 videos for training and 625 videos for testing.

HMDB-51 Human Motion Database dataset provides three train-test splits each consisting of 5100 videos. These clips are labeled with 51 classes of human actions like Clap, Drink, Hug, Jump, Somersault, Throw and many others. Each video has only one action associated with it. The training set for each split has 3570 videos (70 per category) and the test set has 1530 videos (30 per category). The clips have a frame rate of 30 fps.

Hollywood2 Human Actions dataset consists of 1707 video clips collected from movies. These clips are labeled with 12 classes of human actions - AnswerPhone, DriveCar, Eat, FightPerson, GetOutCar, HandShake, HugPerson, Kiss, Run, SitUp, SitDown and StandUp. Some videos have multiple actions associated with them. The training set has 823 videos and the testing set has 884 videos.

All the videos in the datasets were resized to 224×224 resolution and fed to a GoogLeNet model trained on the ImageNet dataset. The last convolutional layer of size $7 \times 7 \times 1024$ was used as an input to our model.

4.2 TRAINING DETAILS AND EVALUATION

In all of our experiments, model architecture and various other hyper-parameters were set using cross-validation. In particular, for all datasets we trained 3-layer LSTM models, where the dimensionality of the LSTM hidden state, cell state, and the hidden layer were set to 512 for both UCF-11 and Hollywood2 and 1024 for HMDB-51. We also experimented with models having one LSTM layer to five LSTM layers, but did not observe any significant improvements in model performance. For the attention penalty coefficient we experimented with values 0, 1, 10. While reporting results, we have set the weight decay penalty to 10^{-5} and use dropout (Srivastava et al.,

Table 1: Performance on UCF-11 (acc %), HMDB-51 (acc %) and Hollywood2 (mAP %)

Model	UCF-11	HMDB-51	Hollywood2
Softmax Regression (full CNN feature cube)	82.37	33.46	34.62
Avg pooled LSTM (@ 30 fps)	82.56	40.52	43.19
Max pooled LSTM (@ 30 fps)	81.60	37.58	43.22
Soft attention model (@ 30 fps, $\lambda = 0$)	84.96	41.31	43.91
Soft attention model (@ 30 fps, $\lambda = 1$)	83.52	40.98	43.18
Soft attention model (@ 30 fps, $\lambda = 10$)	81.44	39.87	42.92

(a) $\lambda = 0$
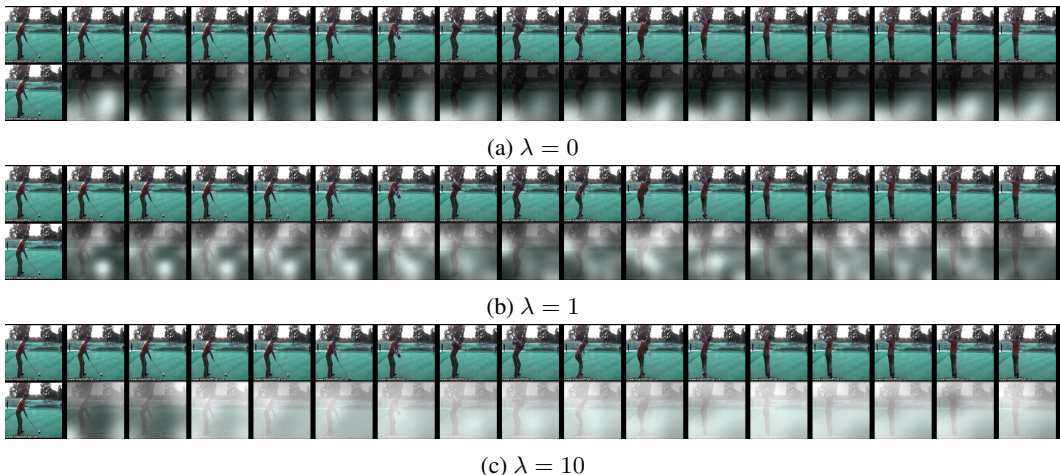

(b) $\lambda = 1$

(c) $\lambda = 10$

Figure 3: Variation in the model's attention depending on the value of attention penalty λ. The white regions are where the model is looking and the brightness indicates the strength of focus. Setting $\lambda = 0$ corresponds to the model that tends to select a few locations and stay fixed on them. Setting $\lambda = 10$ forces the model to gaze everywhere, which resembles average pooling over slices.

2014) of 0.5 at all non-recurrent connections. All models were trained using Adam optimization algorithm (Kingma & Ba, 2015) for 15 epochs over the entire datasets. However, we found that Adam usually converged after 3 epochs. Our implementation is based in Theano (Bastien et al., 2012) which also handles the gradient computation and our code is available at `https://github.com/kracwarlock/action-recognition-visual-attention`.

For both training and testing our model takes 30 frames at a time sampled at fixed fps rates. We split each video into groups of 30 frames starting with the first frame, selecting 30 frames according to the fps rate, and then moving ahead with a stride of 1. Each video thus gets split into multiple 30-length samples. At test time, we compute class predictions for each time step and then average those predictions over 30 frames. To obtain a prediction for the entire video clip, we average the predictions from all 30 frame blocks in the video.

4.2.1 BASELINES

The softmax regression model uses the complete $7 \times 7 \times 1024$ feature cube as its input to predict the label at each time-step t, while all other models use only a 1024-dimensional feature slice as their input. The average pooled and max pooled LSTM models use the same architecture as our model except that they do not have any attention mechanism and thus do not produce a location softmax. The inputs at each time-step for these models are obtained by doing average or max pooling over the $7 \times 7 \times 1024$ cube to get 1024 dimensional slices, whereas our soft attention model dynamically weights the slices by the location softmax (see Eq. 5).

4.3 QUANTITATIVE ANALYSIS

Table 1 reports accuracies on both UCF-11 and HMDB-51 datasets and mean average precision (mAP) on Hollywood2. Even though the softmax regression baseline is given the complete $7 \times 7 \times 1024$ cube as its input, it performs worse than our model for all three datasets and worse than all

Table 2: Comparison of performance on HMDB-51 and Hollywood2 with state-of-the-art models

Model		HMDB-51 (acc %)	Hollywood2 (mAP %)
Spatial stream ConvNet	(Simonyan & Zisserman, 2014)	40.5	-
Soft attention model	(Our model)	41.3	43.9
Composite LSTM Model	(Srivastava et al., 2015)	44.0	-
DL-SFA	(Sun et al., 2014)	-	48.1
Two-stream ConvNet	(Simonyan & Zisserman, 2014)	59.4	-
VideoDarwin	(Fernando et al., 2015)	63.7	73.7
Multi-skIp Feature Stacking	(Lan et al., 2014)	65.1	68.0
Traditional+Stacked Fisher Vectors	(Peng et al., 2014)	66.8	-
Objects+Traditional+Stacked Fisher Vectors (Jain et al., 2015)		71.3	66.4

(a) Correctly classified as "cycling"   (b) Correctly classified as "walking with a dog"
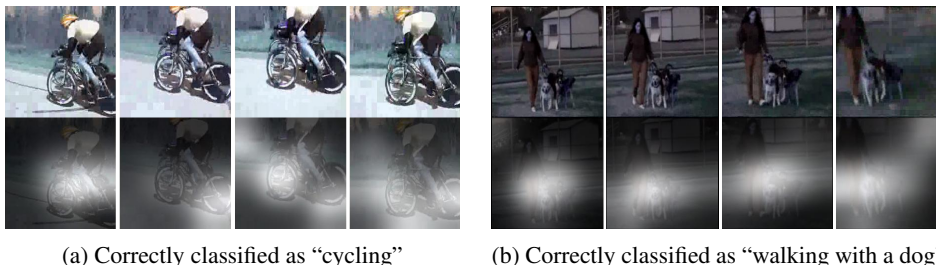
Figure 4: Attention over time. The model learns to look at the relevant parts - the cycle frame in (a) and the human and the dogs in (b)

(a) Incorrectly classified as "diving"
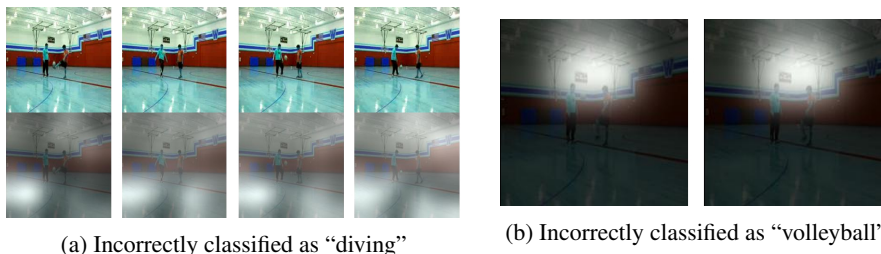
(b) Incorrectly classified as "volleyball"

Figure 5: Video frames for a few time-steps for an example of soccer played on a basketball court. Different glimpses can result in different predictions. Best viewed in color.

models in the case of HMDB-51 and Hollywood2. The results from Table 1 demonstrate that our attention model performs better than both average and max pooled LSTMs.

We next experimented with doubly stochastic penalty term λ (see Eq. 7). Figure 3a shows that with no attention regularization term, $\lambda = 0$, the model tends to vary its attention less. Setting $\lambda = 1$ encourages the model to further explore different gaze locations. The model with $\lambda = 10$ looks everywhere (see Fig. 3c), in which case its behavior tends to become similar to the average pooling case. Values in between these correspond to dynamic weighted averaging of the slices. The models with $\lambda = 0$ and $\lambda = 1$ perform better than the models with $\lambda = 10$.

In Table 2, we compare the performance of our model with other state-of-the-art action recognition models. We do not include UCF-11 here due to the lack of standard train-test splits. We have divided the table into three sections. Models in the first section use only RGB data while models in the second section use both RGB and optical flow data. The model in the third section uses both RGB, optical flow, as well as object responses of the videos on some ImageNet categories. Our model performs competitively against deep learning models in its category (models using RGB features only), while providing some insight into where the neural network is looking.

4.4 QUALITATIVE ANALYSIS

Figure 4 shows some test examples of where our model attends to on UCF-11 dataset. In Fig. 4a, we see that the model was able to focus on parts of the cycle, while correctly recognizing the activity as
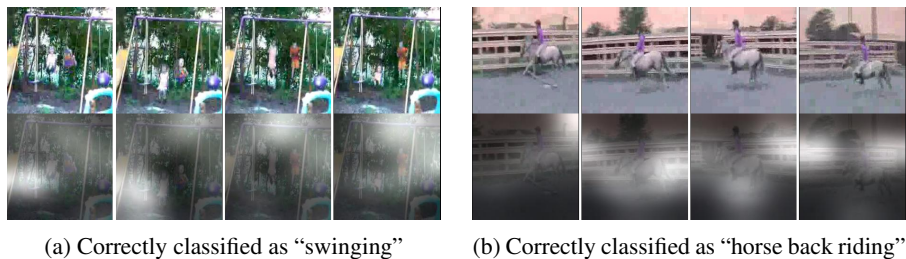
(a) Correctly classified as "swinging"   (b) Correctly classified as "horse back riding"

Figure 6: Video frames where the model pays more attention to the background compared to the foreground and still classifies them correctly

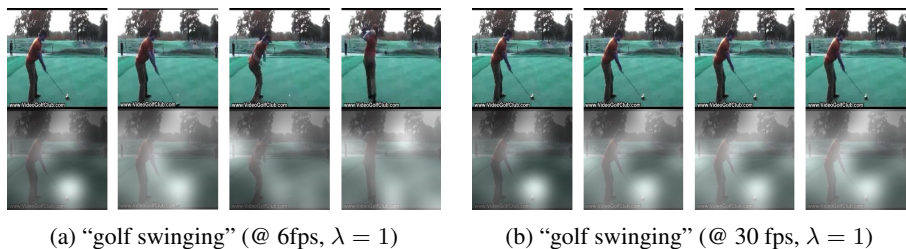(a) "golf swinging" (@ 6fps, $\lambda = 1$)   (b) "golf swinging" (@ 30 fps, $\lambda = 1$)

Figure 7: The model's focus of attention visualized over four equally spaced timesteps at different fps rates. (a) plays faster and when the ball is hit and the club disappears, the model searches around to find them. (b) plays slower and the model stays focused on the ball and the club.

(a) Correctly classified as "Pushup"   (b) Correctly classified as "Kiss"

(c) Inorrectly classified as "Somersault"   (d) Incorrectly classified as "Hit"
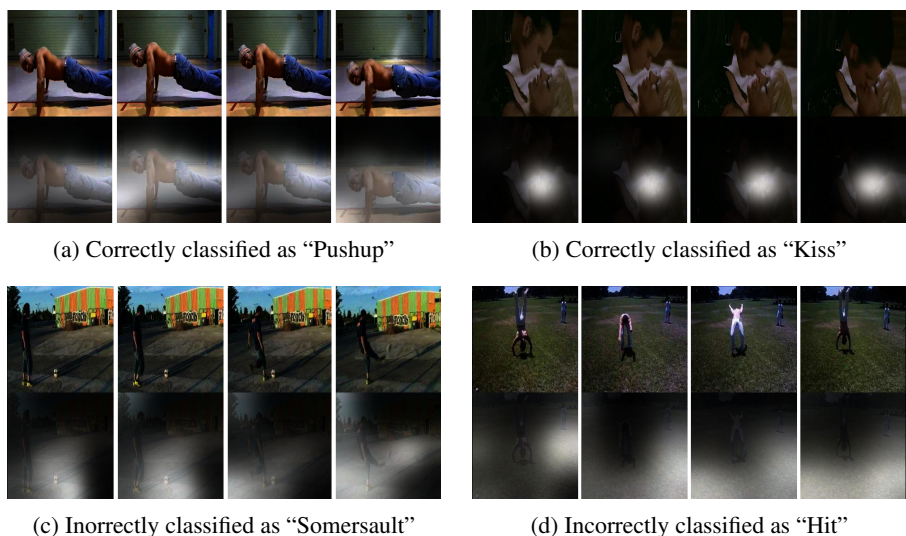
Figure 8: Visualization of the focus of attention for four videos from HMDB-51 and Hollywood2 datasets over time. The white regions are where the model is looking and the brightness indicates the strength of focus.

"cycling". Similarly, in Fig. 4b, the model attends to the dogs and classifies the activity as "walking with a dog".

We can also better understand failures of the model using the attention mechanism. For example, Fig. 5a shows that the model mostly attends to the background like the light blue floor of the court. The model incorrectly classifies the example as "diving". However, using a different manually specified glimpse, as shown in Fig. 5b, the model classifies the same example as "volleyball spiking". It is quite interesting to see that we can better understand the success and failure cases of this deep attention model by visualizing where it attends to.[1]

The model does not always need to attend to the foreground. In many cases the camera is far away and it may be difficult to make out what the humans are doing or what the objects in the frames are. In these cases the model tends to look at the background and tries to infer the activity from the information in the background. For example, the model can look at the basketball court in the

---

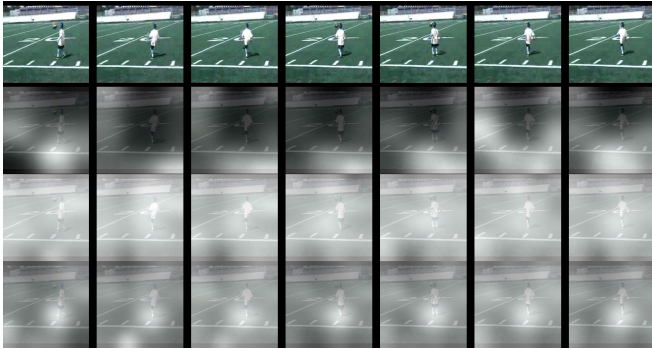[1] All the figures are from our best performing models with $\lambda = 0$ unless otherwise mentioned.

Figure 9: (**First**) The original video frames for a "soccer juggling" example from UCF-11 (**Second**) Glimpse of model with $\lambda = 1$ overlayed on the frames; predicted incorrectly as "tennis swinging" (**Third**) Randomly initialized glimpse overlayed on the frames; predicted incorrectly as "tennis swinging" (**Fourth**) The first glimpse at which the action is correctly predicted as "soccer juggling", overlayed on the frames

background and predict the action being performed. Thus, depending on the video both foreground and background might be important for activity recognition. Some examples are shown in Fig. 6, where the model appears to look everywhere.

It is also interesting to observe that in some cases, the model is able to attend to important objects in the video frames and attempts to track them to some extent in order to correctly identify the performed activity. In Fig. 7b, the video is sampled at 30fps and subsequent frames are almost identical. In this case the model stays focused on the golf ball, club, and the human. However, when we change the sampling rate to 6fps, as shown in Fig. 7a, we find that the video frames change quickly. The model now remains focused on the ball before it disappears. After the person hits the ball, we see that the model tries to look at other places, possibly to track the ball and the golf club.

We next examined the model's performance on the HMDB-51 dataset.[2] In Fig. 8a the model attempts to focus on the person performing push-ups to recognize "Pushup" activity. In Fig. 8c the model classifies the example of "KickBall" incorrectly as "Somersault" despite attending to the location where the action is happening. In some cases, however, the model fails to even attend to the relevant location (see Fig. 8d). For Hollywood2, Fig. 8b shows an example of a short clip belonging to the "Kiss" action. It appears that the model correctly anticipates that a kiss is going to take place and attempts to focus on the region between the man and the woman.

In our final set of experiments, we have tried to examine some failure cases of our attention mechanism. As an example, Fig. 9 shows a test video clip of "soccer juggling" (top row). Our model focuses on the white boundaries of the field (second row), while incorrectly recognizing the activity as "tennis swinging". To see whether we can potentially correct the model's mistake by forcing it to look at the relevant locations, we took a trained model and initialized the location softmax weights to uniform random numbers between the minimum and maximum in the original model. The model's glimpse in this case is shown in the third row of Fig. 9. We next optimized only the softmax weights, or the location variables, for this specific example of "soccer juggling" to find the glimpse for which the model would predict it correctly. All the other model parameters were kept fixed. Note that this only changes the sequences of glimpses, or where the model attends to, and not the model itself. It is interesting to see that in order to classify this video clip correctly, the glimpse the model learns (the fourth row of Fig. 9) tends to focus on the soccer player's legs.

5 CONCLUSION

In this paper we developed recurrent soft attention based models for action recognition and analyzed where they focus their attention. Our proposed model tends to recognize important elements in video frames based on the action that is being performed. We also showed that our model performs better than baselines which do not use any attention mechanism. Soft attention models, though impressive, are still computationally expensive since they still require all the features to perform dynamic pooling. In the future, we plan to explore hard attention models as well as hybrid soft and hard attention approaches which can reduce the computational cost of our model, so that we can potentially scale to larger datasets like UCF-101 and the Sports-1M dataset. These models can also be extended to the multi-resolution setting, in which the attention mechanism could also choose to focus on the earlier convolutional layers in order to attend to the lower-level features in the video frames.

---

[2]More examples of our model's attention are available in Appendix A and at
http://www.cs.toronto.edu/~shikhar/projects/action-recognition-attention.

REFERENCES

J. Ba, R. Grosse, R. Salakhutdinov, and B. Frey. Learning wake-sleep recurrent attention models. In *NIPS*, 2015a.

J. Ba, V. Mnih, and K. Kavukcuoglu. Multiple object recognition with visual attention. *ICLR*, 2015b.

D. Bahdanau, K. Cho, and Y. Bengio. Neural machine translation by jointly learning to align and translate. *ICLR*, 2015.

F. Bastien, P. Lamblin, R. Pascanu, J. Bergstra, I. J. Goodfellow, A. Bergeron, N. Bouchard, D. Warde-Farley, and Y. Bengio. Theano: new features and speed improvements. *CoRR*, abs/1211.5590, 2012.

J. Deng, W. Dong, R. Socher, L.-J. Li, K. Li, and F.-F. Li. Imagenet: A large-scale hierarchical image database. In *CVPR*, 2009.

J. Donahue, L. A. Hendricks, S. Guadarrama, M. Rohrbach, S. Venugopalan, K. Saenko, and T. Darrell. Long-term recurrent convolutional networks for visual recognition and description. In *CVPR*, 2015.

B. Fernando, E. Gavves, J. Oramas, A. Ghodrati, and T. Tuytelaars. Modeling video evolution for action recognition. In *CVPR*, 2015.

A. Graves, N. Jaitly, and A.-r. Mohamed. Hybrid speech recognition with deep bidirectional LSTM. In *2013 IEEE Workshop on Automatic Speech Recognition and Understanding*, pp. 273–278. IEEE, 2013.

S. Hochreiter and J. Schmidhuber. Long short-term memory. *Neural Computation*, 9(8):1735–1780, 1997.

M. Jaderberg, K. Simonyan, A. Zisserman, and K. Kavukcuoglu. Spatial transformer networks. *CoRR*, abs/1506.02025, 2015.

M. Jain, J. C. v. Gemert, and C. G. M. Snoek. What do 15,000 object categories tell us about classifying and localizing actions? In *CVPR*, June 2015.

A. Karpathy, G. Toderici, S. Shetty, T. Leung, R. Sukthankar, and F.-F. Li. Large-scale video classification with convolutional neural networks. In *CVPR*, 2014.

D. P. Kingma and J. Ba. Adam: A method for stochastic optimization. *ICLR*, 2015.

Z.-Z. Lan, M. Lin, X. Li, A. G. Hauptmann, and B. Raj. Beyond gaussian pyramid: Multi-skip feature stacking for action recognition. *CoRR*, abs/1411.6660, 2014.

V. Mnih, N. Heess, A. Graves, and K. Kavukcuoglu. Recurrent models of visual attention. In *NIPS*, 2014.

Y. Netzer, T. Wang, A. Coates, A. Bissacco, B. Wu, and A. Y. Ng. Reading digits in natural images with unsupervised feature learning. In *NIPS Workshop on Deep Learning and Unsupervised Feature Learning 2011*, 2011.

J. Y.-H. Ng, M. J. Hausknecht, S. Vijayanarasimhan, O. Vinyals, R. Monga, and G. Toderici. Beyond short snippets: Deep networks for video classification. In *CVPR*, 2015.

X. Peng, C. Zou, Y. Qiao, and Q. Peng. Action recognition with stacked fisher vectors. In *ECCV*, volume 8693, pp. 581–595. Springer, 2014.

S. Ren, K. He, R. B. Girshick, X. Zhang, and J. Sun. Object detection networks on convolutional feature maps. *CoRR*, abs/1504.06066, 2015.

R. A. Rensink. The dynamic representation of scenes. *Visual Cognition*, 7(1-3):17–42, 2000.

K. Simonyan and A. Zisserman. Two-stream convolutional networks for action recognition in videos. In *NIPS*. 2014.

N. Srivastava, G. E. Hinton, A. Krizhevsky, I. Sutskever, and R. Salakhutdinov. Dropout: a simple way to prevent neural networks from overfitting. *JMLR*, 15(1):1929–1958, 2014.

N. Srivastava, E. Mansimov, and R. Salakhutdinov. Unsupervised learning of video representations using LSTMs. *ICML*, 2015.

L. Sun, K. Jia, T.-H. Chan, Y. Fang, G. Wang, and S. Yan. DL-SFA: deeply-learned slow feature analysis for action recognition. In *CVPR*, 2014.

I. Sutskever, O. Vinyals, and Q. V. V. Le. Sequence to sequence learning with neural networks. In *NIPS*. 2014.

C. Szegedy, W. Liu, Y. Jia, P. Sermanet, S. Reed, D. Anguelov, D. Erhan, V. Vanhoucke, and A. Rabinovich. Going deeper with convolutions. In *CVPR*, 2015.

S. Venugopalan, H. Xu, J. Donahue, M. Rohrbach, R. J. Mooney, and K. Saenko. Translating videos to natural language using deep recurrent neural networks. *CoRR*, abs/1412.4729, 2014.

O. Vinyals, A. Toshev, S. Bengio, and D. Erhan. Show and tell: A neural image caption generator. In *CVPR*, 2015.

R. J. Williams. Simple statistical gradient-following algorithms for connectionist reinforcement learning. *Machine Learning*, 8:229–256, 1992.

R. Wu, S. Yan, Y. Shan, Q. Dang, and G. Sun. Deep image: Scaling up image recognition. *CoRR*, abs/1501.02876, 2015.

K. Xu, J. Ba, R. Kiros, K. Cho, A. C. Courville, R. Salakhutdinov, R. S. Zemel, and Y. Bengio. Show, attend and tell: Neural image caption generation with visual attention. *ICML*, 2015.

L. Yao, A. Torabi, K. Cho, N. Ballas, C. Pal, H. Larochelle, and A. Courville. Describing videos by exploiting temporal structure. *CoRR*, abs/1502.08029, 2015.

S. Yeung, O. Russakovsky, N. Jin, M. Andriluka, G. Mori, and F.-F. Li. Every moment counts: Dense detailed labeling of actions in complex videos. *CoRR*, abs/1507.05738, 2015.

W. Zaremba, I. Sutskever, and O. Vinyals. Recurrent neural network regularization. *CoRR*, abs/1409.2329, 2014.

S. Zha, F. Luisier, W. Andrews, N. Srivastava, and R. Salakhutdinov. Exploiting image-trained CNN architectures for unconstrained video classification. *CoRR*, abs/1503.04144, 2015.

A   ADDITIONAL EXAMPLES

We present some more correctly classified examples from UCF-11, HMDB-51 and Hollywood2 in Fig. 10 and incorrectly classified examples in Fig. 11.

(a) "dive"   (b) "draw_sword"

(c) "climb"   (d) "push"

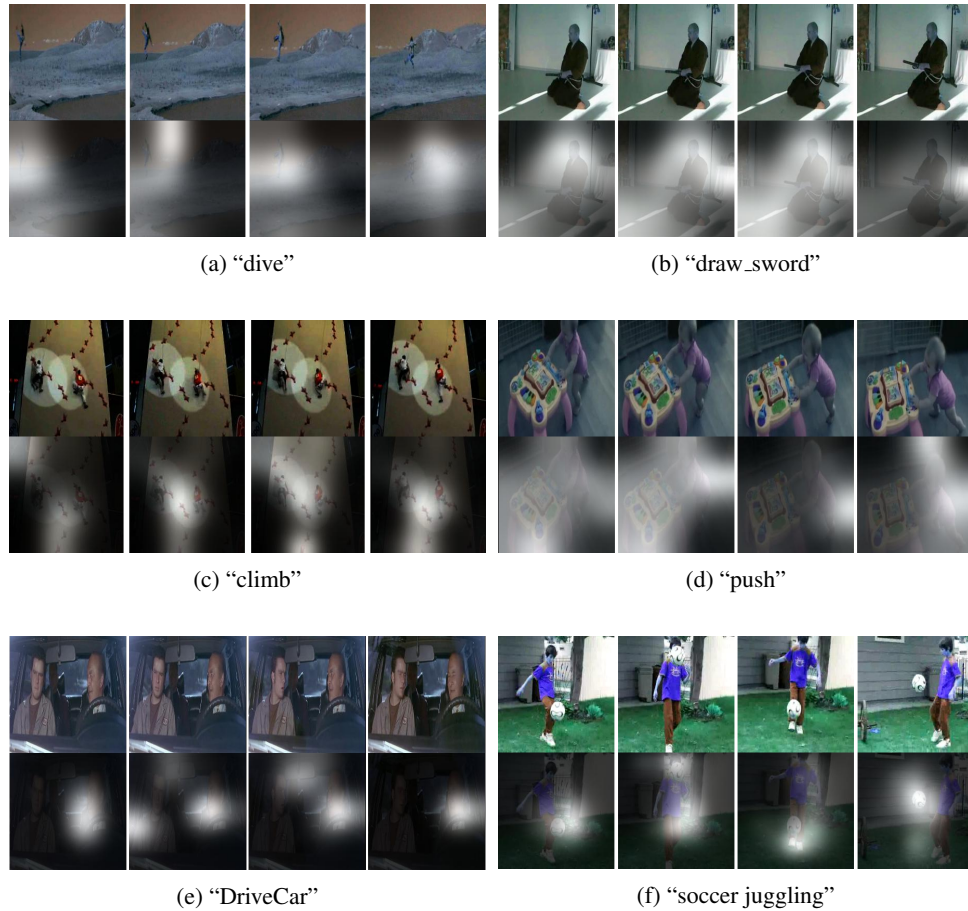(e) "DriveCar"   (f) "soccer juggling"

Figure 10: Correctly classified video frames showing attention over time: The white regions are where the model is looking and the brightness indicates the strength of focus. The model learns to look at relevant parts.

(a) "pour" misclassified as "push"   (b) "laugh" misclassified as "smile"
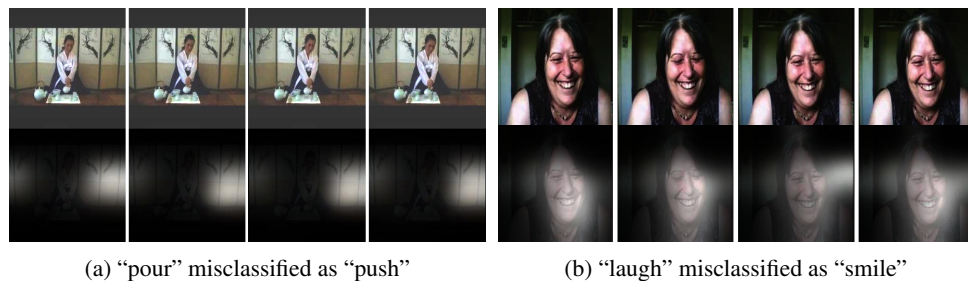
Figure 11: Incorrectly classified video frames showing attention over time: The white regions are where the model is looking and the brightness indicates the strength of focus.